

The role of conductive pathways in the conductivity and rheological behavior of poly(methyl methacrylate)-graphite composites

Xianhu Liu,¹ Yamin Pan,¹ Xiaoqiong Hao,¹ Kun Dai,² Dirk W. Schubert¹

¹Institute of Polymer Materials, Friedrich-Alexander University Erlangen-Nuremberg, Martensstr 7, 91058, Erlangen, Germany

²College of Materials Science and Engineering, National Engineering Research Center for Advanced Polymer Processing Technology, Zhengzhou University, Zhengzhou 450002, China

Correspondence to: X. Liu (E-mail: xianhu.liu@fau.de) and D. Schubert (E-mail: dirk.schubert@fau.de)

ABSTRACT: Up to now, research on the dynamic process of conductive network formation has tended to focus on composite particles with one-dimensional geometry, such as carbon black and carbon nanotubes. However, studies on this subject based on fillers with two-dimensional structure, such as graphite, are rare in the literature. In this work, the dynamic percolation and rheological properties of poly(methyl methacrylate) (PMMA)-graphite composites under an electric field were investigated. The activation energies of conductive network formation and polymer matrix mobility were calculated from the temperature dependence of the percolation time and the zero-shear viscosity. It was found that the activation energy calculated from the zero-shear viscosity was not influenced by the electric field in the concentration range investigated, but the electric field had an effect on the activation energy calculated from the percolation time. This finding emphasizes that the electrical and rheological properties have different physical origins. © 2016 Wiley Periodicals, Inc. *J. Appl. Polym. Sci.* **2016**, *133*, 43810.

KEYWORDS: amorphous; composites; conducting polymers; rheology; self-assembly

Received 18 November 2015; accepted 17 April 2016

DOI: 10.1002/app.43810

INTRODUCTION

Conductive polymer composites (CPC) with conductive filler concentration lower than its percolation threshold exhibit an insulator-conductor transition behavior under isothermal annealing at temperatures above the glass-transition temperature or melting point of the matrix; this phenomenon is called dynamic percolation.¹⁻¹⁰ Conductive network formation in CPCs during dynamic percolation is attributed to self-assembly of the conductive particles. This process can be considered as a thermodynamic nonequilibrium, in which the formation of a conductive network is highly dependent on the annealing temperature, annealing time, and filler loading and on the application of an electric field.³⁻⁷

So far, research on the dynamic process of conductive network formation under an electric field has mostly focused on composites with conductive fillers such as carbon black (CB), carbon fibers (CF), or carbon nanotubes (CNT).¹⁻¹⁰ This is attributed to the fact that the geometries of these fillers can be considered as one-dimensional (1D), and these fillers favor rearrangement under an electric field in the molten state,^{11,12} relative to the fillers with two-dimensional (2D) geometry such as graphite or graphene.¹²⁻¹⁸ For example, Martin *et al.*³

observed the alignment of CNT networks in an epoxy matrix under different electric fields. Zhang *et al.*⁵ and Su *et al.*⁶ investigated the electric-field-controlled formation of conductive pathways in a polycarbonate (PC) melt. They all found that the dynamic percolation time was shortened with increasing electric field intensity. However, to the best of our knowledge, few studies have reported on the influence of 2D particles on the dynamic process of conductive network formation under an electric field.⁷

Compared to the 1D particles, graphite particles have a relatively larger scale, and their movement in the molten state will be less pronounced. Therefore, a large knowledge gap still needs to be filled with respect to the influence of an electric field and process characteristics such as annealing temperature and filler type on the resulting timescales for an insulator-conductor transition of the composites. In this work, we examined the effect of an electric field and annealing temperature to find out how these parameters affect the time required for the insulator-conductor transition in the poly(methyl methacrylate) (PMMA)-graphite composites with a low filler level. The activation energies of conductive network formation as well as PMMA mobility were also investigated and compared.

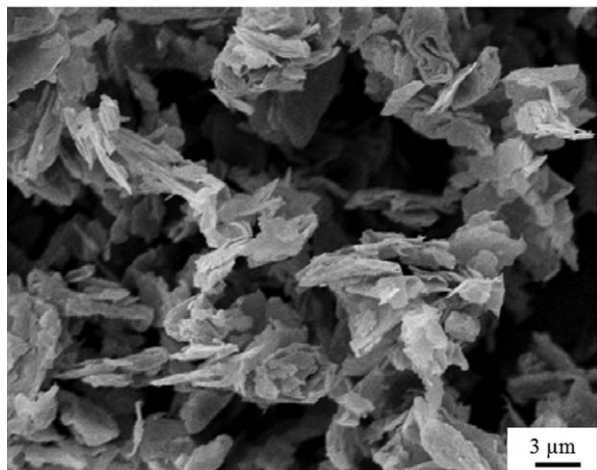


Figure 1. SEM image of graphite UF2.

EXPERIMENTAL

Materials

Commercially available PMMA Plexiglas 7N with a density of 1.19 g cm^{-3} supplied by Evonik Röhm GmbH (Darmstadt, Germany) was used as the matrix material. The weight-average molar mass of PMMA is 98.7 kg mol^{-1} , and the glass-transition temperature was determined to be $109 \text{ }^\circ\text{C}$. Graphite UF2 from GK Kropfmühl (Hauzenberg, Germany) with a density of 2.31 g cm^{-3} was used as the conductive particle. The conductivity of the graphite determined in a powder conductivity measuring cell at 1700 bar was 13 S/cm . The scanning electron microscopy (SEM) in Figure 1 revealed the plate dimensions of a few microns and a mean height of a stack to be about $0.2 \text{ } \mu\text{m}$. The mean equivalent particle diameter was measured with laser light diffraction to be $5.1 \text{ } \mu\text{m}$.

Sample Preparation

The PMMA-graphite composites were prepared via melt mixing using a corotating twin-screw extruder Leistritz LSM 30/34 GL (Nuernberg, Germany) at $202 \text{ }^\circ\text{C}$ with a screw speed of 16 rpm. The extruded composite material was cooled with water and then pelletized. The extruded composite materials were then compression-molded to 2-mm-thick disks with a diameter of 25 mm. They were first preheated at $200 \text{ }^\circ\text{C}$ for 5 min with vacuum and then hot-pressed at 100 bar for 2 min and then cooled to room temperature for 10 min. Prior to the sample preparation and the measurements, the materials were dried at $80 \text{ }^\circ\text{C}$ under vacuum for at least 24 h.

Characterization

The morphology of PMMA composites was examined using SEM (Carl Zeiss Microscopy, Munich, Germany), with an accelerating voltage of 3 kV. The samples were fractured in liquid nitrogen to obtain undeformed fracture surfaces, and the surfaces were then coated with gold using Sputter Coater S150B from Edwards (West Sussex, UK).

For simultaneous rheological and electrical measurements, the setup of a stress-controlled shear rheometer Gemini from Malvern Instruments (Worcestershire, UK) was modified [Figure 2(a)]. The original steel rotor was changed into a highly con-

ductive brass. The upper end of the rotor was made of poly(ether ether ketone) (PEEK) in order to insulate the rotor from the driving unit of the rheometer [Figure 2(b)]. The two electrodes [Figure 2(a)] were connected to a Picoammeter 6487 from Keithley (Ohio, USA). It was checked that the upper plate wire did not affect the rheological quantities. The DC resistance R of the composite was recorded simultaneously during the experiment at a constant voltage (1, 5 or 10 V). The experiment was carried out under a nitrogen atmosphere. Before starting any experiment, an equilibration time of 5 min in the measuring chamber at the chosen temperature was allowed. The electrical conductivity σ was calculated from R using the following equation:

$$\sigma = d/\pi r^2 R \quad (1)$$

where d and r are the thickness and radius of the sample, respectively. Rheological measurements were performed in oscillatory shear. The frequency dependence of the complex viscosity was investigated in a frequency range between 0.01 and 100 rad/s at a stress amplitude of 50 Pa.

RESULTS AND DISCUSSION

The morphology of the PMMA composites was characterized by SEM. As an example, the structure of the PMMA composite containing 10 vol % of graphite is shown in Figure 3. It can be seen that the graphite is homogeneously distributed in the polymer matrix. Additionally, there are no obvious contacts of graphite particles to generate the conductive pathways.

In a CPC, the conductive particles are separated by energy barriers (polymer molecules), and the tunnel effect becomes relevant in modifying the percolation model.^{7,14} At high annealing temperature (above the melting temperature of the polymer matrix), the relaxation of the polymer chains facilitates the reorganization of the dispersed conductive particles, promoting the formation of conductive pathways and decreasing the percolation threshold. Figure 4(a) shows a typical example of the time-dependent conductivity of PMMA composites with different filler loadings under an electric field of 50 V/cm at $200 \text{ }^\circ\text{C}$. Interestingly, the conductivity of composites with 10 vol % graphite first remains constant with increasing annealing time, and then a tremendous increase of more than five orders of magnitude

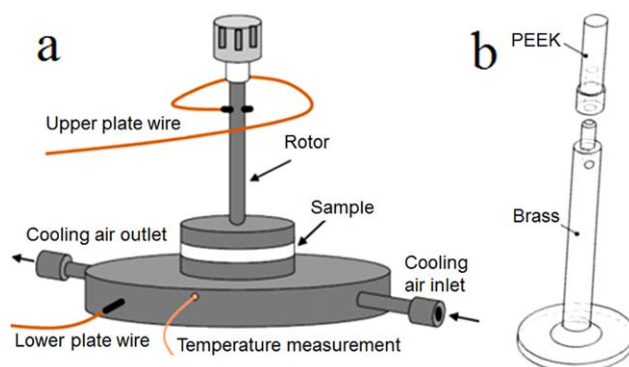


Figure 2. (a) Setup for simultaneous measurements of electrical and rheological properties and (b) principle of the rotor. [Color figure can be viewed in the online issue, which is available at wileyonlinelibrary.com.]

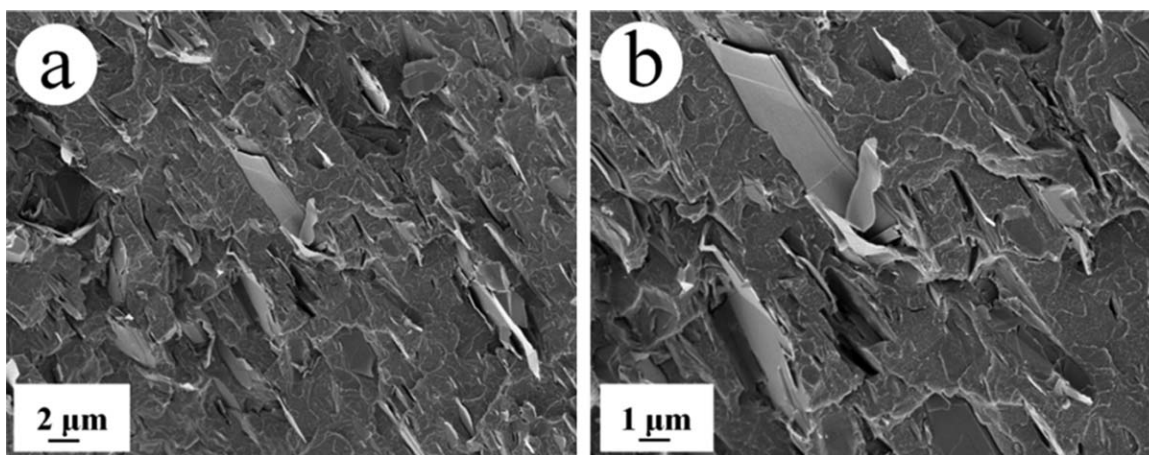


Figure 3. SEM images of PMMA composite filled with 10 vol % graphite: (a) low and (b) high magnification.

when reaching a critical annealing time (t_p) is clearly observed. This phenomenon is a typical insulator–conductor transition.

Figure 4(b) shows the conductivity at different annealing times of PMMA composites with different filler loadings under an electric field of 50 V/cm at 200 °C. Concerning the initial conductivity values (0 h), one can determine that the (static) percolation threshold of PMMA–graphite composites is between 10 and 15 vol %, which is in good agreement with the SEM result. However, after annealing (>0.5 h), the (dynamic) percolation threshold shifts to a low value (less than 10 vol %).

The insulator–conductor transition can be influenced by the annealing temperature, electric field, and filler concentration. To better understand this behavior, we chose the PMMA composites with 10 vol % graphite to study the effect of annealing temperature and electric field. Figure 5 shows the typical example of the time-dependent conductivity of PMMA composites under different electric fields and annealing temperatures. Similarly, there exists an insulator–conductor transition behavior. As expected, at a given time, a high conductivity is obtained under a large electric field intensity or a high annealing temperature.^{1–10} The critical annealing time is defined as the percolation time t_p , which can be

used to estimate the difficulty of the initial conductive pathway formation. The effect of the electric field on the percolation time is depicted in the Figure 6(a). Here, the percolation time is a mean value from at least three individual specimens. It can be found that, at the same annealing temperature, the percolation time decreases with increasing electric field. In the presence of the electric field, the conductive particles can be electrically polarized.^{3–7} This effect induces a torque to orient the particles parallel to the field direction, forming more effective conductive pathways. Hence, with increasing electric field, more conductive pathways are constructed, resulting in the reduction of percolation time. Additionally, the value of percolation time decreases with increasing annealing temperature. This is attributed to the high annealing temperature giving rise to a low viscosity of the polymer matrix (Figure 7), resulting in a good conducting connection.⁷

Recently, a relationship between the percolation time ($\ln t_p$) and the electric field E was proposed by Su *et al.*⁶:

$$\ln t_p = kE + b \quad (k < 0) \quad (2)$$

According to eq. (2), b represents the percolation time ($\ln t_p$) without application of an electric field. Therefore, we can get the percolation time without application of an electric field.

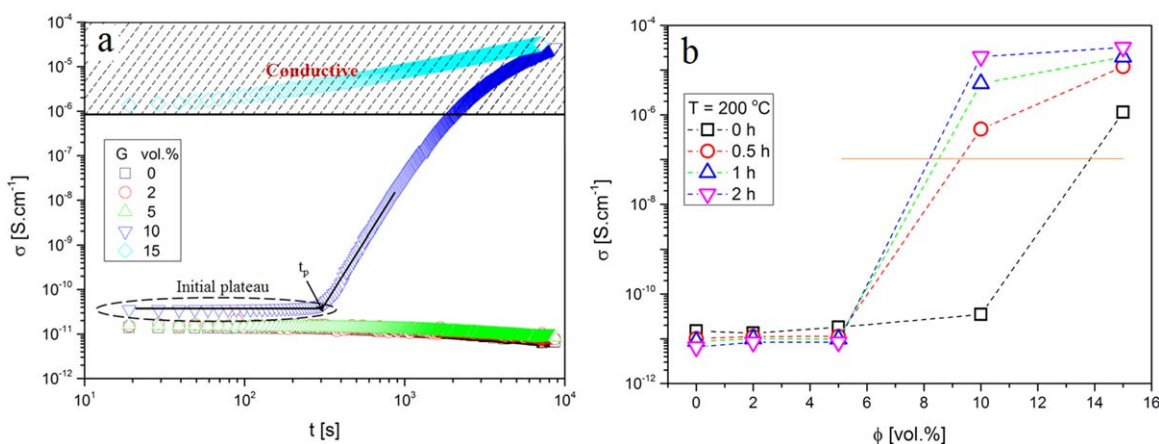


Figure 4. (a) Time-dependent conductivity and (b) conductivity at different annealing times of PMMA composites with different filler loadings (50 V/cm, 200 °C). The arrow in (a) indicates the percolation time t_p of the sample. [Color figure can be viewed in the online issue, which is available at wileyonlinelibrary.com.]

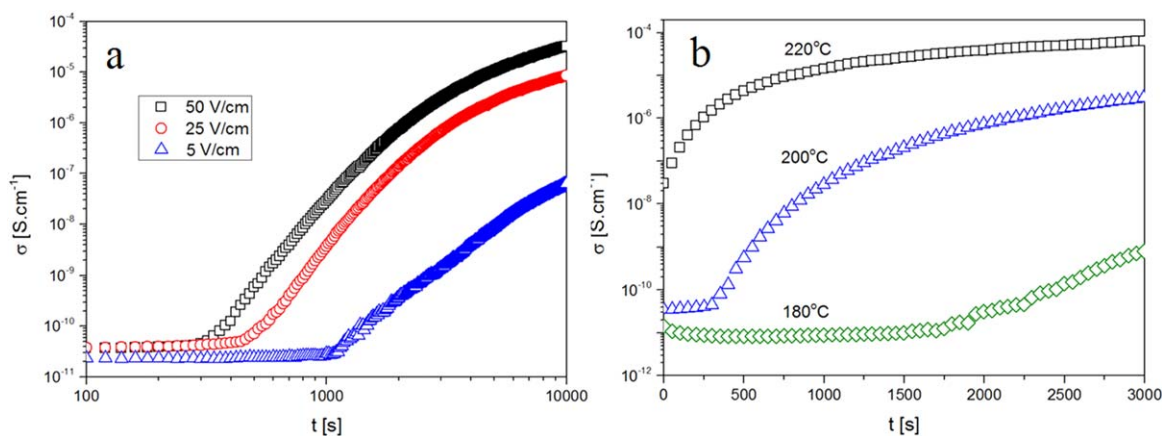


Figure 5. Time-dependent conductivity of PMMA composites under different (a) electric fields (200 °C) and (b) annealing temperatures (50 V/cm). [Color figure can be viewed in the online issue, which is available at wileyonlinelibrary.com.]

Here, these values are very close to the percolation time at 5 V/cm [Figure 6(b)], indicating that a small electric field has a limited effect on the dynamic percolation. To confirm this, the composite samples for room-temperature electrical conductivity measurements were annealed at 200 °C for 3000 s without application of an electric field in a compression molding (150 bar). It is found that the electrical conductivity of the composites increases to about 2.0×10^{-9} S/cm, and this value is very close to the value of the composite samples at 5 V/cm. This result indicates that the dynamic percolation has already occurred before 3000 s. Unfortunately, the exact percolation time is difficult to determine in this situation. Nevertheless, eq. (2) provides a possible method to design and develop CPCs with desirable electrical conductivity at low filler concentration via changing the electric field or annealing time.

The Arrhenius equation can be used to calculate the activation energy E_a of conductive network formation in a polymer melt.⁹ In our case, the Arrhenius equation [eq. (3)] can be expressed as

$$\ln t_p = \ln A - E_a/RT \quad (3)$$

where R is the gas constant, A is an arbitrary constant, and T is the absolute temperature. As shown in Figure 6(b), $\ln t_p$ and

b hold a good linear relationship with the inverse of the annealing temperature. The value of the activation energy for b was estimated by eq. (3) to be about 144 kJ/mol. This value is the same as the activation energy at an electric field of 5 V/cm, indicating that a small electric field has no effect on the activation energy, which is consistent with the above result. Nevertheless, as the electric field increases from 5 V/cm to 25 V/cm, the activation energy decreases from 144 kJ/mol to 124 kJ/mol. However, taking into account the standard deviation, the activation energy remains nearly invariable with the further increase of the electric field up to 50 V/cm. This result indicates that the activation energy of conductive network formation could be changed by an electric field with a certain intensity, which is confined by both an upper critical value and a lower one.⁶ Moreover, it is proved that the change in the interfacial interaction of polymer and filler particle could result in the variation of activation energy.⁹ Therefore, it also indicates that the electric field causes some changes in the interfacial interaction between polar PMMA chains and graphite particles. However, if the polymer matrix is a nonpolar polymer, the activation energy would remain almost the same under various electric fields.^{4,7}

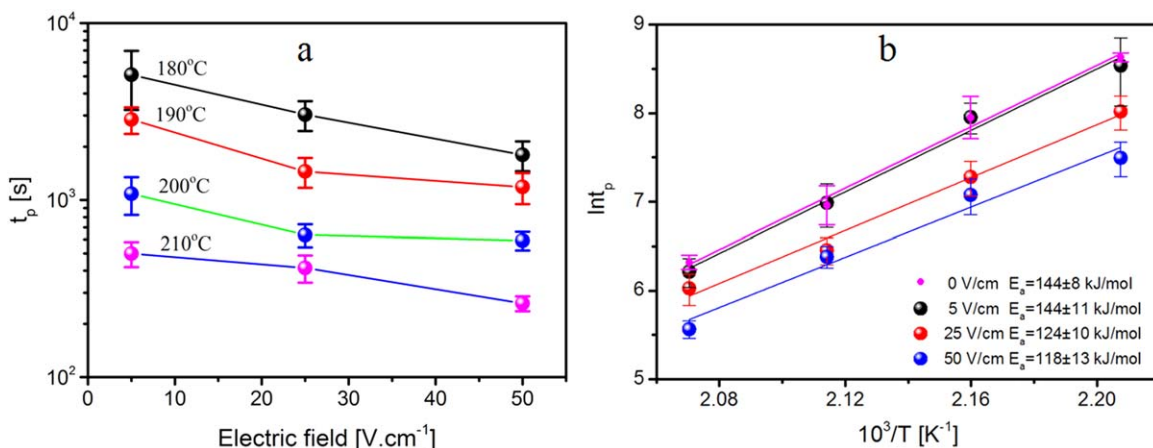


Figure 6. (a) Percolation time t_p vs. electric field at different annealing temperatures and (b) Arrhenius plots of $\ln t_p$ vs. the inverse of the annealing temperature. [Color figure can be viewed in the online issue, which is available at wileyonlinelibrary.com.]

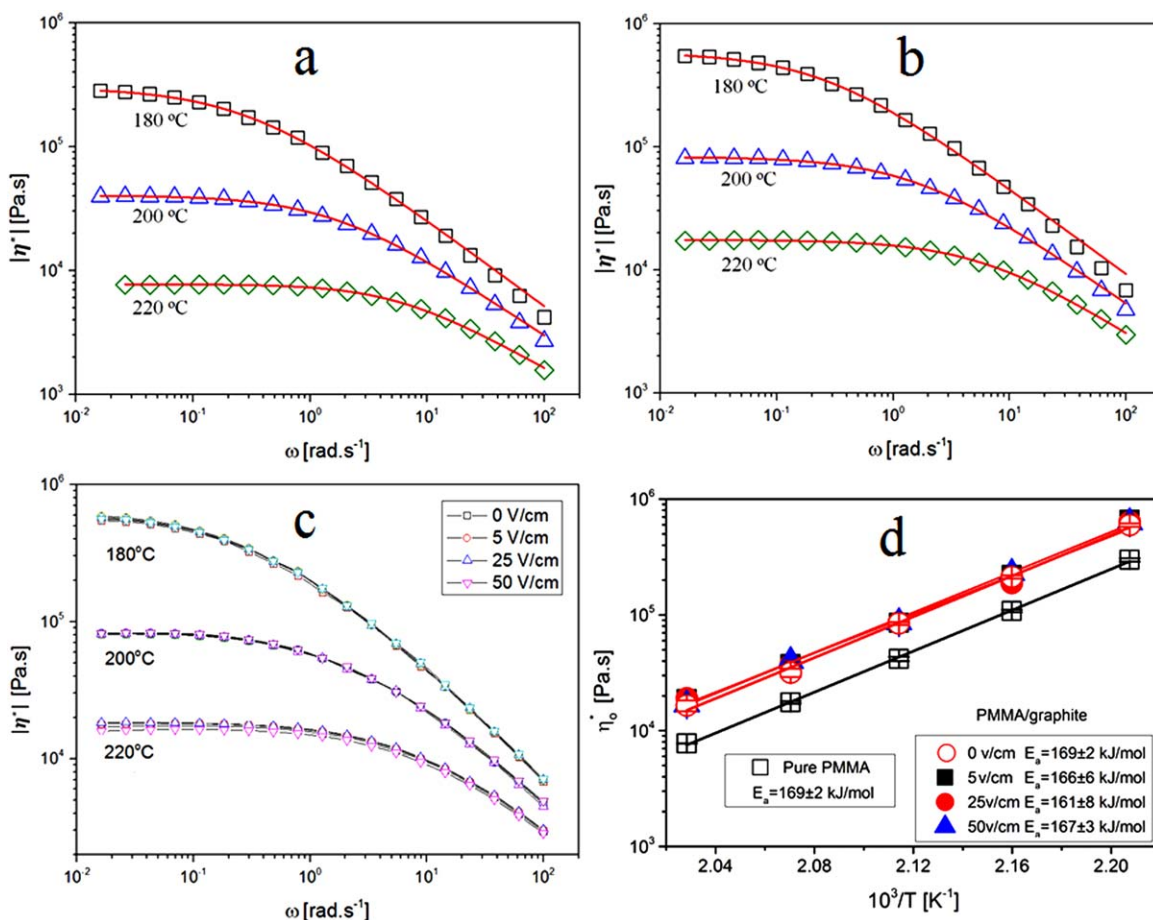


Figure 7. Angular frequency dependence of the complex viscosity at various temperatures: (a) pure PMMA, (b) PMMA composites, and (c) PMMA composites under different electric fields. (d) Arrhenius plots of zero-shear viscosity η_0 vs. the inverse of the annealing temperature. The lines in Figure 7(a–c) are fits to eq. (4). [Color figure can be viewed in the online issue, which is available at wileyonlinelibrary.com.]

In order to discuss the kinetics of the percolation process, the mobility of the PMMA polymer matrix was measured at different temperatures. From Figure 7(a,b), it is observed that the viscosity increases with the incorporation of filler, and it decreases with increasing temperature. Moreover, the viscosity increases with decreasing frequency to a constant value, called the zero-shear viscosity η_0 . The Arrhenius plots of zero-shear viscosity against the annealing temperature can reveal the flow activation energy of PMMA mobility. Therefore, the Carreau equation is introduced to extrapolate zero-shear viscosity:

$$|\eta^*| = \frac{\eta_0}{\left[1 + \left(\frac{\omega}{\omega_0}\right)^m\right]^n} \quad (4)$$

where ω_0 is the critical angular frequency at which the viscosity function begins to decrease; n and m are the fit parameters. Generally, as the filler concentration increases, the activation energy of polymer matrix mobility increases in the composites. The increased activation energy is attributed to the presence of the interaction between filler and polymer matrix.¹⁹ However, as shown in Figure 7(d), the activation energy from zero-shear viscosity remains unchanged (169 kJ/mol) for pure PMMA and PMMA composites with 10 vol % graphite. This result indicates

that the activation energy of PMMA mobility is not influenced by the filler in the concentration range investigated, which is attributed to the poor filler–matrix adhesion of graphite particles and PMMA matrix.

Figure 7(c) shows the angular frequency dependence of the complex viscosity at various temperatures for PMMA composites under different electric fields. It is clear that the applied electric field makes no difference to the complex viscosity in the frequency range investigated. This result can also be confirmed by the activation energy calculated by the zero-shear viscosity [Figure 7(d)], in which the activation energy is almost the same in all the electric fields investigated. Moreover, these values are very close to the activation energy of zero-shear viscosity without application of the electric field (169 kJ/mol). Hence, the impact of an electric field on the flow activation energy is negligible. This is attributed to the viscosity of a composite melt being given by the combined network, that is, entanglements of the polymer chain network, the filler aggregate network, and the interaction between the polymer entanglement and filler aggregate networks.^{20–23} As is well known, the electrical conductivity is strongly dependent on the mean distance between the particles or agglomerates, and the mean distance between particles or agglomerates in a composite is decreased by increasing

the filler volume concentration.^{24,25} In our case, the occurrence of conductive network formation can be explained by the agglomeration of graphite particles at a fixed concentration. The mechanism underlying the electric field and annealing temperature can be understood as follows. At first the graphite composites did not show any connected conductive pathways (see Figure 3), so their electrical conductivity was very low and therefore presented a plateau in Figures 4 and 5. During annealing, on one hand, Brownian motion allowed the conductive particles to aggregate, leading to an increase in agglomerate size to enhance the conductivities.^{25–27} On the other hand, the relaxation of the polymer chains under annealing facilitated the reorganization of the dispersed particles.²⁷ Furthermore, when an electric field is imposed, the conductive particles can be electrically polarized. This effect can orient the conductive particles parallel to the electric field direction, forming more effective conductive pathways.^{3–7} Because of the larger geometry of the graphite particles, there was no doubt that small movements were sufficient to bring two graphite particles close enough to enable the transfer of electrons.⁷ Thus, at a certain annealing time, the agglomerates interconnected and formed a pathway through the polymer matrix. Additionally, the turning point caused by the applied electric field was also counteracted by the viscosity of the polymer matrix. The increase in the annealing temperature also accelerated the relaxation of the polymer molecules. Thus, this effect was more pronounced for composites with lower viscosity. Therefore, at a larger electric field or high annealing temperature, the insulator–conductor transition became more obvious.

For 1D-particle-filled CPC, the dynamic percolation is more sensitive to temperature, in comparison to the viscoelasticity of the composites. The difference can be understood by the formation of different networks, that is, the conductive network for charge carrier transport and the combined network for mechanical momentum to transfer.²⁸ In earlier studies, Cao *et al.*²³ and Zhang *et al.*²⁹ investigated the dynamic percolation of CB-filled high-density polyethylene and CNT-filled polypropylene copolymer, respectively. They agreed that the activation energy of percolation time (E_{a-t_p}) was higher than the activation energy of zero-shear viscosity of filled polymer composites ($E_{a-\eta_c}$). Otherwise, E_{a-t_p} approached the activation energy of zero-shear viscosity of the polymer matrix ($E_{a-\eta_p}$) or $E_{a-\eta_c}$.^{9,10} As shown in Figure 7(d), $E_{a-\eta_c}$ regardless of the electric field is very close to $E_{a-\eta_p}$, but is higher than E_{a-t_p} [Figure 6(b)], which is in disagreement with the speculations in the references.^{9,10,23,29} These results indicate that the conductive network of the composites is less related to the interaction between PMMA molecules and graphite particles. Meanwhile, our results confirm that the movement of graphite particles is more difficult than that of 1D particles in a polymer matrix,^{30–32} which is in good agreement with the small variation of activation energy values of conductive network formation and our speculation. The main reason can be attributed to the different geometries of the particles. Benedict *et al.*³³ proved for single-wall carbon nanotubes that their polarization strongly depended on their geometrical parameters. In the direction of the axes, the polarization was much more pronounced than in the radial direction. Therefore,

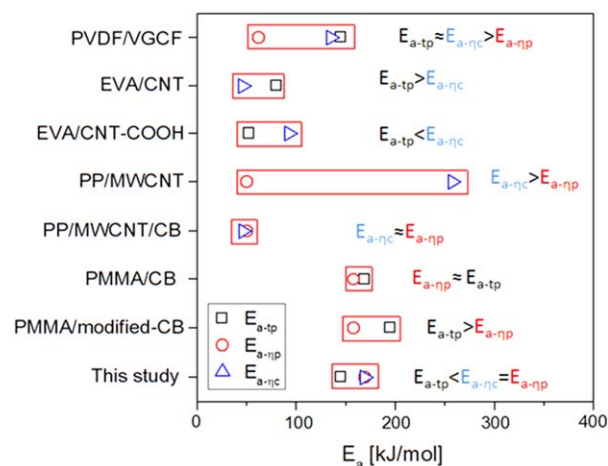


Figure 8. E_a of η_0 and t_p comparison with the data from the literature. The polymer matrixes are PMMA for ref. 9, Poly(vinylidene fluoride) (PVDF) for ref. 10, ethylene vinyl acetate (EVA) for refs. 8 and 19, and polypropylene (PP) for ref. 29. Insert: E_a of η_0 and t_p vs. electric field. [Color figure can be viewed in the online issue, which is available at wileyonlinelibrary.com.]

the effect of graphite with a plate geometry under the same electric field will be less pronounced than for the 1D particle. Finally, to better understand the variation of activation energy in CPCs with different fillers, activation-energy values calculated by the percolation time and zero-shear viscosity are plotted to compare with some results reported in the literature (Figure 8).^{8–10,19,29} Those results further indicate that the filler types, such as filler geometry and surface polarity, greatly affect the activation-energy values.^{7–10,34,35}

CONCLUSIONS

In this work, the insulator–conductor transition and the rheological properties of PMMA–graphite composites below the percolation threshold were investigated. The percolation time required to reach the insulator–conductor transition under quiescent conditions was studied as a function of electric field intensity as well as annealing temperature. It was found that the electrical conductivity was increased with increasing annealing time in the molten state. For example, the increase of the electrical conductivity at 200 °C and 50 V/cm was more than five orders of magnitude. This was attributed to the aggregation of freely dispersed graphite into conductive pathways. In particular, at a larger electric field or high annealing temperature, this behavior became more obviously due to the enhancement of Brownian motion of the conductive particles and the lower viscosity of the polymer matrix. Moreover, the activation energy for the network formation process was calculated from the temperature dependence of the percolation time. It was found that the electric field had an effect on the activation energy for conductive network formation. Furthermore, the frequency response of the rheological properties of the pure PMMA and the composites was studied at different temperatures in the linear-viscoelastic regime. It was found that the flow activation energy calculated from the zero-shear viscosities at different temperatures of the PMMA matrix was not influenced by the filler in the concentration range and electric field investigated.

This finding emphasized the differences in network formation with respect to electrical or rheological properties as both properties had different physical origins.

ACKNOWLEDGMENTS

The authors are grateful to Dr. Yaping Ding for the SEM images. X.L. and Y.P. acknowledge the China Scholarship Council for funding the scholarship.

REFERENCES

1. Cao, Q.; Song, Y. H.; Tan, Y. Q.; Zheng, Q. *Carbon* **2010**, *48*, 4268.
2. Li, W. L.; Zhang, Y. Q.; Yang, J. J.; Zhang, J.; Niu, Y. H.; Wang, Z. G. *ACS Appl. Mater. Interfaces* **2012**, *4*, 6468.
3. Martin, C. A.; Sandler, J. K. W.; Windle, A. H.; Schwarz, M. K.; Bauhofer, W.; Schulte, K.; Shaffer, M. S. P. *Polymer* **2005**, *46*, 877.
4. Tai, X. Y.; Wu, G. Z.; Yui, H.; Asai, S.; Sumita, M. *Appl. Phys. Lett.* **2003**, *83*, 3791.
5. Zhang, C.; Zhu, J.; Ouyang, M.; Ma, C. A. *Appl. Phys. Lett.* **2009**, *94*, 111915.
6. Su, C.; Xu, L. H.; Yan, R. J.; Chen, M. Q.; Zhang, C. *Mater. Chem. Phys.* **2012**, *133*, 1034.
7. Pang, H.; Chen, C.; Zhang, Y. C.; Ren, P. G.; Yan, D. X.; Li, Z. M. *Carbon* **2011**, *49*, 1980.
8. Zhang, Y.; Zheng, C. D.; Pang, H.; Tang, J. H.; Li, Z. M. *Compos. Sci. Technol.* **2012**, *72*, 1875.
9. Wu, G. Z.; Asai, S.; Zhang, C.; Miura, T.; Sumita, M. *J. Appl. Phys.* **2000**, *88*, 1480.
10. Zhang, C.; Wang, L.; Wang, J. L.; Ma, C. A. *Carbon* **2008**, *48*, 2053.
11. Schaefer, D. W.; Justice, R. S. *Macromolecules* **2007**, *40*, 8501.
12. Goedel, A.; Marmur, A.; Kasaliwal, G. R.; Poetschke, P.; Heinrich, G. *Macromolecules* **2011**, *44*, 6094.
13. Wu, G.; Lin, J.; Zheng, Q.; Zhang, M. Q. *Polymer* **2006**, *47*, 2442.
14. Garzùn, C.; Palza, H. *Compos. Sci. Technol.* **2014**, *99*, 117.
15. Sheng, P.; Sichel, E. K.; Gittleman, J. I. *Phys. Rev. Lett.* **1978**, *40*, 1197.
16. Mironov, V. S.; Kim, J. K.; Park, M.; Lim, S.; Cho, W. K. *Polym. Test.* **2007**, *26*, 547.
17. Chen, G. H.; Wu, C. L.; Weng, W. G.; Wu, D. J.; Yan, W. L. *Polymer* **2003**, *44*, 1781.
18. Dweiri, R.; Sahari, J. *J. Power Sources* **2007**, *171*, 424.
19. Bao, Y.; Pang, H.; Xu, L.; Cui, C. H.; Jiang, X.; Yan, D. X.; Li, Z. M. *RSC Adv.* **2013**, *3*, 24185.
20. Pan, Y. Z.; Cheng, H. K. F.; Li, L.; Chan, S. H.; Zhao, J. H.; Juay, Y. K. *J. Polym. Sci., Polym. Phys.* **2010**, *48*, 2238.
21. Zhang, X.; Yan, X.; He, Q.; Wei, H.; Long, J.; Guo, J.; Gu, H.; Yu, J.; Liu, J.; Ding, D.; Sun, L.; Wei, S.; Guo, Z. *ACS Appl. Mater. Interfaces* **2015**, *7*, 6125.
22. Zhu, J.; Wei, S.; Li, Y.; Sun, L.; Haldolaarachchige, N.; Young, D. P.; Southworth, C.; Khasanov, A.; Luo, Z.; Guo, Z. *Macromolecules* **2011**, *44*, 4382.
23. Cao, Q.; Song, Y. H.; Tan, Y. Q.; Zheng, Q. *Polymer* **2009**, *50*, 6350.
24. Liu, X. H.; Krücker, J.; Zheng, G. Q.; Schubert, D. W. *Compos. Sci. Technol.* **2014**, *100*, 99.
25. Liu, X. H.; Krücker, J.; Zheng, G. Q.; Schubert, D. W. *ACS Appl. Mater. Interfaces* **2013**, *5*, 8857.
26. Liu, X. H.; Pan, Y. M.; Zheng, G. Q.; Schubert, D. W. *Compos. Sci. Technol.* **2016**, *128*, 1.
27. Pan, Y. M.; Liu, X. H.; Hao, X. Q.; Starý, Z.; Schubert, D. W. *Eur. Polym. J.* **2016**, *78*, 106.
28. Zhou, J. F.; Song, Y. H.; Shangguan, Y. G.; Zheng, Q. *J. Appl. Polym. Sci.* **2008**, *110*, 2001.
29. Zhang, S. M.; Lin, L.; Deng, H.; Gao, X.; Bilotti, E.; Peijs, T.; Zhang, Q.; Fu, Q. *Colloid Polym. Sci.* **2012**, *290*, 1393.
30. Song, Y. H.; Cao, Q.; Zheng, Q. *Colloid Polym. Sci.* **2012**, *290*, 1837.
31. Song, Y. H.; Xu, C. F.; Zheng, Q. *Soft Matter* **2014**, *10*, 2685.
32. Tan, Y.; Yin, X.; Chen, M.; Song, Y.; Zheng, Q. *J. Rheol.* **2011**, *55*, 965.
33. Benedict, L. X.; Loui, S. G.; Cohen, M. V. *Phys. Rev. B* **1995**, *52*, 8541.
34. Zhang, C.; Zhu, J.; Ouyang, M.; Ma, C.; Sumita, M. *J. Appl. Polym. Sci.* **2009**, *114*, 1405.
35. Zhang, Y. C.; Pang, H.; Dai, K.; Huang, Y. F.; Ren, P. G.; Chen, C.; Li, Z. M. *J. Mater. Sci.* **2012**, *47*, 3713.

SGML and CITI Use Only
DO NOT PRINT

